Microphthalmia, persistent hyperplastic hyaloid vasculature and lens anomalies following overexpression of VEGF-A$_{188}$ from the αA-crystallin promoter

Catrin S. Rutland,[1] Christopher A. Mitchell,[2] Muneeb Nasir,[3] Moritz A. Konerding,[4] Hannes C.A. Drexler[5]

[1]*School of Biomedical Sciences, Medical School, University of Nottingham, Derby Road, Nottingham, United Kingdom;* [2]*Centre for Molecular Biosciences, School of Biomedical Sciences, University of Ulster, Coleraine, United Kingdom;* [3]*Department of Obstetrics and Gynaecology, University of Nottingham, City Hospital, Nottingham, United Kingdom;* [4]*Department of Anatomy, Johannes Gutenberg-University Mainz, Mainz, Germany;* [5]*Max Planck Institute for Heart and Lung Research, W.G. Kerckhoff Institute, Bad Nauheim, Germany*

Purpose: During growth of the embryonic eye, dose- and site-specific expression of heparin-binding growth factors is critical for the formation of an appropriate vascular supply. Overexpression of vascular endothelial growth factor-A$_{188}$ (VEGF-A$_{188}$), a strongly heparin-binding, endothelial-specific mitogen, leads to severe disturbance of vascular and overall ocular morphology. This study aimed to evaluate the effects of VEGF-A$_{188}$ overexpression on growth of ocular tissue components.

Methods: Stereological and immunohistochemical methods were employed to identify the vascular profiles, ocular tissue proportions, and cell types in VEGF-A$_{188}$ transgenic mice and compare them with wild-type mice.

Results: In VEGF-A$_{188}$ transgenic mice, both lens tissue and total ocular volume were reduced, whereas cross-sectional areas of hyaloid blood vessels, retina, iris, and optic stalk tissues were significantly increased compared to wild-type mice. Endothelial and pericyte cell numbers in the hyaloid vasculature of transgenic mice were increased three fold, with pericytes assuming their characteristic extraluminal position.

Conclusions: Overexpression of VEGF-A$_{188}$ in the murine lens results in microphthalmia, in addition to hypertrophy and persistence of the hyaloid vasculature. This is similar to the human disorder persistent hyperplastic primary vitreous (PHPV). The murine model is a useful, experimental paradigm for investigation of this condition.

The concentration and distribution of matrix-bound growth factors is critical during cellular differentiation and for appropriate tissue patterning in embryogenesis [1]. For instance, in the developing eye, retinal differentiation and growth is dependent on signals emanating in a temporally restricted pattern from the primitive lens. Ocular morphology is, therefore, intimately associated with the rapid expansion of the lens, which throughout embryogenesis, is supported by a tightly adherent circulation system termed the hyaloid vasculature (HV) [1]. During this rapid phase of growth, the lens produces a variety of peptide growth factors that serve to support localized tissue expansion and the temporally restricted maintenance of the HV [1]. Among these factors are FGF2, PDGF-β, and VEGF-A [1-3]. In the case of the vascular endothelium, VEGF-A levels and the cellular expression pattern is normally tightly regulated, with modest alterations, result-

ing in embryonic lethal phenotypes [4-7]. These studies reinforce the critical nature of VEGF-A expression in the development and maintenance of the vascular system. However, tissue-restricted expression of VEGF-A and its major isoforms in the eye, due to the nonlethal nature of resultant phenotypes, allows a fuller appreciation of the consequences of misexpression of isoforms of this critical growth factor, particularly in the pathogenesis of ocular diseases.

During normal murine HV development, VEGF-A is principally secreted by lens epithelial cells located at the lens equator, and transcripts of the gene are downregulated perinatally [8]. VEGF-A$_{188}$, one specific isoform of VEGF-A, is transcribed from all eight exons of the gene and strongly binds heparin-associated residues [9-11]. VEGF-A$_{188}$ is immediately matrix-bound following secretion [12] and is most highly expressed in the lung [13]. During embryonic development, the soluble isoforms of VEGF-A$_{120}$ and VEGF-A$_{164}$ are the major isoforms expressed [13] with lens capsule heparin-sulphate proteoglycans (HSPG) potentially acting as a VEGF-A reservoir [14]. A number of ocular pathologies are characterized by deregulated neovascularization, and these conditions correlate with increased levels of total VEGF-A [15-17] - most specifically the VEGF-A$_{165}$ isoform [1,18]. However, the role of VEGF-A$_{188}$, the most tightly bound VEGF-A isoform, during development and in the pathophysiology of ocular disease remains to be determined.

Correspondence to: Dr. Christopher A. Mitchell, Centre for Molecular Biosciences, School of Biomedical Sciences, University of Ulster, Cromore Rd, Coleraine, BT52 1SA, United Kingdom; Phone: +44 (0)28 70324089; FAX: +44 (0)28 70324965; email: ca.mitchell@ulster.ac.uk

Dr. Drexler is now at the Universität Würzburg, Institut für Medizinische Strahlenkunde und Zellforschung - MSZ, Versbacherstr. 5, D-97078 Würzburg, Germany

In this study, we analyze and interpret an ocular phenotype in transgenic mice resulting from lens-specific overexpression of VEGF-A$_{188}$. The evidence from this study supports the hypothesis that the microphthalmia and lens anomalies are a direct result of perturbations in the vascular morphology of the HV, while the retinal hypertrophy may be a direct consequence of the retinal ganglion cell responses to this growth factor. These results have particular relevance for human fetal conditions characterized by ocular vascular abnormalities, such as retinopathy of prematurity (ROP) and persistent hyperplastic primary vitreous (PHPV), establishing the experimental paradigm that vascular malformation can result in the gross ocular pathologies characteristic of these conditions.

METHODS

Animal model: The transgene construction, genotyping, and analysis of VEGF-A$_{120}$, VEGF-A$_{164}$, and VEGF-A$_{188}$ mice is described elsewhere [19]. In brief, the open reading frame cDNA of murine VEGF-A$_{188}$ was cloned in frame into a CPV2 construct [1], and transgenic mice were derived according to standard methodologies. The mice generated by these methods demonstrated lens-specific expression of the VEGF-A$_{188}$ protein from the αA-crystallin promoter. In our study, adult female C57Bl6J mice (8 weeks old) and heterozygous αA-crystallin-VEGF-A$_{188}$ transgenic males were housed in a 12 h:12 h light-dark schedule and were allowed to mate. T females were examined and the presence of a vaginal plug was defined as embryonic day 0.5 (E0.5; n=19 pregnant dams). The females were euthanized and their gravid uteri were carefully dissected free. After amnionectomy, the fetuses were delivered, euthanized, and eyes were enucleated. One eye from each embryo was fixed in 10% buffered formal saline (BFS; pH 7.4) overnight, subsequently embedded in araldite, and sectioned for stereological analysis. The contralateral eye was fixed in 4% paraformaldehyde for 30 min, embedded in paraffin, sectioned (5 μm) and prepared for either immunohistochemical or TUNEL staining or fixed in 2.5% glutaraldehyde in cacodylate buffer for ultrastructural studies. All experiments adhered to Home Office (National) and institutional guidelines (comparable to those published by the Institute for Laboratory Animal Research, *Guide for the Care and Use of Laboratory Animals*).

Ocular stereology: A total of five wild-type mice and six transgenic littermates were randomly selected from the total population of collected fetuses. Following fixation, eyes were processed, critically orientated in a mold, and embedded in araldite. Serial sections (0.5 μm thick) were cut at 50 μm intervals through the eye, sections placed onto slides and subsequently stained with 2% toluidine blue. A three-stage stereological analysis was performed to determine (1) ocular volume, (2) tissue and vascular fractions, and (3) vascular morphometry using systematic random sampling [20,21]. Light microscopic images were obtained using an Olympus microscope and electronic images were captured with the aid of an Olympus T4040 digital camera. Each section was visualized and stereological analysis performed with the aid of the "QProdit" computer imaging software (Leica Imaging Systems, Cambridge, UK).

Ocular volume: The perimeter of each eye section was traced and the area calculated. Cross-sectional areas from individual sections were multiplied by 50 (to take into account that sections were cut at 50 μm intervals) and subsequently summed to determine fetal ocular volume.

Tissue fraction: Two systematically random views [21] of each eye section were collected, stored, and analyzed with the aid of a 96-point grid layout. The ocular tissues were assigned to one of 11 tissue-type groups based on their location and histological phenotype: retina, lens stroma, cornea, vitreous humor, aqueous humor, iris, lens hemorrhage, lenticular hyaloid vasculature, retinal hyaloid vasculature, optic stalk, and nonocular tissue (includes the sclera and eyelid).

Vascular morphometry: A photomicrograph of each section containing HV was analyzed by tracing around each blood vessel. Vessels within the "broken lines" were included within the count, whereas vessels crossing the solid lines were excluded. Blood vessel lengths, cross-sectional areas, diameters, and volumes were calculated using the tissue fraction and ocular volume data based on the following formulas:

$$\text{Vol all BV (mm}^3) = \text{BV fraction in eye} \times \text{Volume of eye (mm}^3)$$

$$\text{Vol of BV (mm}^3) = \frac{\text{Vol all BV (mm}^3) \times \text{Area of BV (}\mu\text{m}^2)}{\text{Area of BV (}\mu\text{m}^2)}$$

$$\text{Lv} = 2 \times \text{Q/A} = \frac{\text{Vol of BV} \times \text{Number of BV} \times 10^6}{\text{Forbidden lines (cm)} \times \text{Number of sections}}$$

$$\text{Length of BV in eye (metres)} = \frac{(\text{Vol of eye (mm}^3)/1000) \times \text{Lv}}{100}$$

$$\text{BV Cross-sectional area (}\mu\text{m}^2) = \frac{\text{Volume of BV (mm}^3)}{\text{Length of BV (metres)}/1000}$$

Vol = volume, BV = blood vessel, Lv = amount of blood vessels within sample area

Measurement of corneal thickness in neonatal mice: Heterozygous male transgenic mice were crossed with wild-type female mice, and the eyes from resulting litters (P2) were enucleated, fixed in formalin overnight, and embedded in araldite. Sections were cut (5 μm thick) through the geometric center of the eye (containing the optic nerve; located using light-microscopy), placed onto microscope slides, and stained with hematoxylin and eosin. The phenotype of each pup was identified from its ocular morphology as either transgenic or wild-type. The number of cell layers in the cornea was counted manually under a final magnification of 200X. A nonparametric Friedman test was utilized to ensure that there were no significant differences between wild-type embryos selected from litters containing VEGF-A$_{188}$ mice, and one-way analysis of variance (ANOVA) with post-hoc testing (SPSS v11.0) was used to compare wild-type and transgenic mouse corneas.

Transmission electron microscopy: Ocular samples were embedded in Epon Araldite (TAAB, Aldermaston, Berks, UK), and semithin sections (about 0.8 μm thickness) were cut from blocks on a Reichert-Jung Ultracut-E microtome (Leica Microsystems, Nussloch, Germany), stained with 2% toluidine blue, and examined prior to further ultrastructural analy-

sis. Ultrathin sections of gold interference color (about 80 nm thickness) were cut, and contrasted with uranyl acetate and lead citrate. Sections were viewed using a JEOL JEM-1010 transmission electron microscope (JEOL, Tokyo, Japan) at an accelerating voltage of 80 kV. Electronic images were captured on a Kodak Megaplus camera model 1.6i (Kodak, San Diego, CA).

Scanning Electron Microscopy: Specimens were fixed in Karnovsky's fixative solution (2% paraformaldehyde/2% glutaraldehyde in 0.1 M phosphate buffer; pH 7.4) for 1 h, washed several times with PBS for 15 min each, followed by post fixation with 1% osmium tetroxide in 0.1 M phosphate buffer for 1 h. After rinsing with PBS for a minimum of 15 min, the specimens were dehydrated with a series of graded ethyl alcohols (70% for 15 min, 95% for 15 min. and three changes of 100% for 10 min each). The samples were then dried using hexamethyldisilazane (HMDS; Sigma-Aldrich, UK). After drying, the specimens were mounted on aluminium stubs with adhesive tabs and coated with gold for 3 min using a Polaron (Energy Beam Sciences, Agawam, MA) sputter coater. The specimens were examined on an AMRAY 1000A (Bedford, MA) scanning electron microscope.

Immunohistochemistry: Immunohistochemical detection of VEGF-A (1:100 dilution in PBS; Santa Cruz Biotechnology, Inc, Santa Cruz, CA), heparan sulfate proteoglycan (HSPG, 1:100 dilution in PBS; Upstate Biotechnology, Charlottesville, VA), macrophage cell surface marker F4/80

(1:150 dilution in PBS; Southern Biotechnology, Birmingham, AL) or α-smooth muscle actin antibodies (1:400 dilution in PBS; Sigma) was carried out according to the manufacturer's instructions using the Vectastain (Burlingame, CA), ABC staining method.

Statistical Analysis: Statistical comparisons between groups were assessed using a one-way ANOVA with post-hoc testing, with a $p < 0.05$ considered as significant.

RESULTS

The gross anatomical features in adult VEGF-A$_{188}$ transgenic mice include microphthalmia and bilateral cataracts (Figure 1A,B; insets). The characteristic feature of sections from eyes of late fetal (E18.5) transgenic mice are fused clusters of vascular channels that are closely apposed to the posterior surface of the lens, retinal dysplasia, and corneal thickening (Figure 1B,D). Lens epithelial cells encircled the lens, the characteristic bowing of lens fiber cells was lost (Figure 1D), and vascular invasion frequently led to intralenticular hemorrhage. Ultrastructural investigations (E15.5) revealed that both endothelial cells and pericytes contributed to a hyperplastic hyaloid vasculature on the posterior pole of the lens, with numerous attendant macrophages (Figure 1E-H).

Ocular volume and tissue fraction stereology: Absolute ocular volumes in VEGF-A$_{188}$ transgenic mice were an average of 33% smaller than their control littermates (mean±SEM=1.1791±0.0287 mm^3, transgenic=0.7849±0.1180
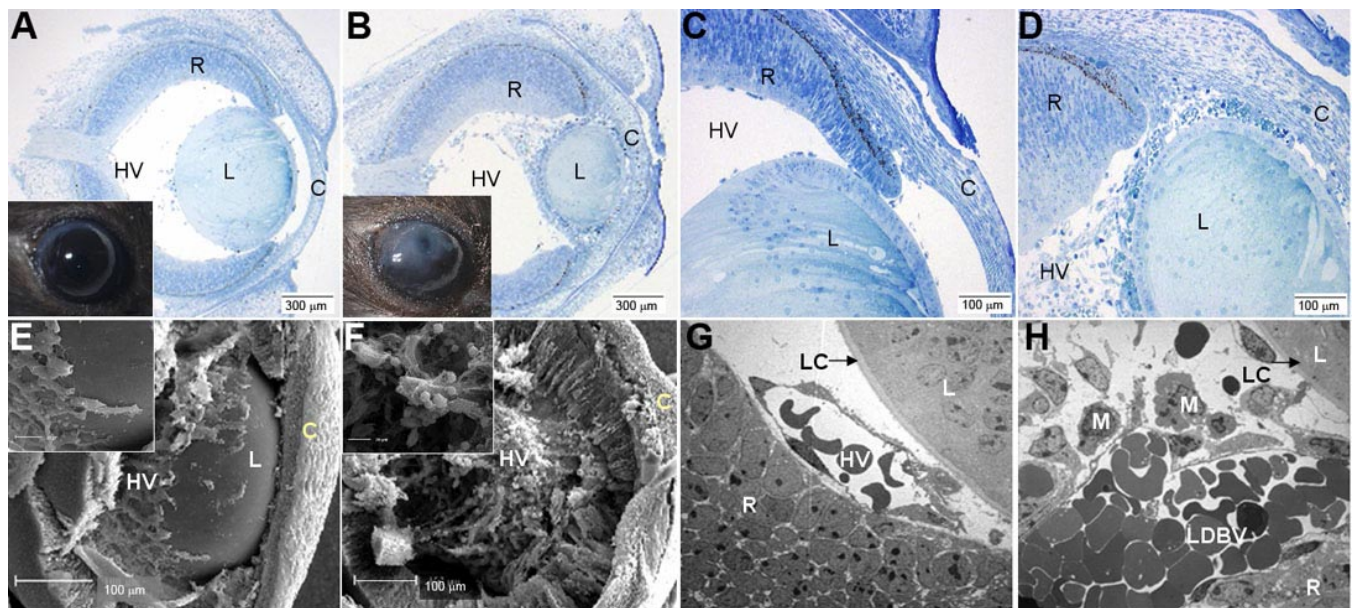

Figure 1. Gross anatomical and microscopic features of VEGF-A$_{188}$ transgenic mice. Representative photomicrographs of toluidine blue-stained sections from E18.5 wild-type (**A**,**C**) and VEGF-A188 transgenic (**B**,**D**) mice. Gross ocular phenotypes of adult wild-type (**A**; inset) and a VEGF-A188 transgenic mouse (**B**; inset), showing conspicuous cataract formation. In VEGF-A188 transgenic mice (B, D), a hypertrophic hyaloid vasculature surrounds a small lens. There is evidence of retinal hypertrophy, particularly in the ganglion cell layer at the top of these micrographs. Scanning electron micrographs of wild-type (**E**) and VEGF-A$_{188}$ transgenic (**F**) mice are shown. The thickened hypertrophic hyaloid vasculature with numerous adherent mononuclear cells in the VEGF-A$_{188}$ transgenic lens (**F**) contrasts with the organized plexus in wild-type mice. Transmission electron micrographs of hyaloid blood vessels in E18.5, wild-type (**G**), and VEGF-A$_{188}$ transgenic mice (**H**). Large diameter vessels(LDBV), with several attendant macrophages (**M**), are conspicuous in VEGF-A$_{188}$ transgenics. In the images, C=cornea, HV=hyaloid vasculature, R=retina, and L=lens.

mm^3; p<0.008; Figure 2A). In late fetal mice, there are two distinct anatomical regions of the hyaloid vasculature: that surrounding the lens (tunica vascular lentis, TVL, which incorporates the papillary membrane anteriorly), and a retinal component (arteria hyaloidea propria, AHP) on the vitreal surface of the inner limiting membrane [22]. Lenticular vessel proportions (TVL) were increased four fold and retinal vessels (AHP) two fold when compared with wild-type eyes (Table 1), with lens hemorrhage only ever being observed in VEGF-A_{188} transgenic mice (6/6 transgenics; 0/5 controls).

The total proportion of lens tissue (stroma plus hemorrhagic tissue) decreased by 39%, whereas lens stromal tissue alone was reduced by 62% in VEGF-A_{188} transgenic mice in comparison to littermate controls. In addition to these conspicuous changes in lens morphology, the fraction of retina, iris, and optic stalk tissue were all significantly increased (Table 1). The fractional proportion of vessels in VEGF-A_{188} transgenic eyes increased in comparison to controls in the AHP (p=0.003), iris (p=0.02), and optic stalk (p=0.01); however, the absolute ocular volumes of these tissue types were not significantly different (Table 1). This indicates that these tissue types were relatively unaffected by the overexpression of VEGF-A_{188}, but they occupied a greater volume in a smaller eye. Additionally, despite having a smaller retinal volume, the proportion of AHP and TVL vessels increases (Table 1), particularly in regions around the lens equator (Figure 1). Perilenticular retinal hypertrophy was a consistent feature of VEGF-A_{188} transgenic mice, and general retinal thickening was a consistent finding (both features observed in five out of six transgenic eyes at E18.5; Table 1). To determine whether this

vascular and retinal hypertrophy is associated with conspicuous HSPG-bound VEGF-A_{188} in the lens capsule and adjacent retinal surface, we performed immunohistochemical analysis on critically oriented specimens from E18.5 mice.

Ocular blood vessel stereology: Although blood vessel length was not significantly altered (p<0.58; Figure 2B), the hyaloid vascular cross-sectional area increased two fold (p<0.0001; Figure 2C) in E18.5 VEGF-A_{188} transgenic mice, resulting in a doubling of total vascular volume (p<0.002; Figure 2D). This increase in cross-sectional area of hyaloid vasculature surrounding the lenses of E18.5 VEGF-A_{188} transgenic mice is particularly conspicuous on the posterior and lateral surfaces of the lens (Figure 1B,D,F,H).

Measurement of corneal thickness in neonatal mice: The non-parametric Friedman test showed that there were no significant differences between wild-type embryos selected from different litters containing VEGF-A_{188} mice (p<0.704; n=45). The number of layers comprising the cornea was significantly increased in the VEGF-A_{188} transgenic mice (15.7±0.99, mean±SEM endothelial cells thick, n=10) in comparison with wild-type mice (12.93±0.50 layers thick, mean±SEM, p<0.033). Despite an increase in the number of corneal layers, the VEGF-A_{188} transgenic eyes did not have an increased corneal thickness in comparison with wild-type mice (p>0.05).

VEGF immunohistochemistry: Specific immunohistochemical staining for VEGF-A was observed in sections from the eyes of E15.5, P1 and adult mice (Figure 3). Weak cytoplasmic staining of the retina, lens stroma, and outer lens capsule was observed in wild-type eyes (Figure 3B,D,F). Strong VEGF-A specific immunostaining was observed in the lens,
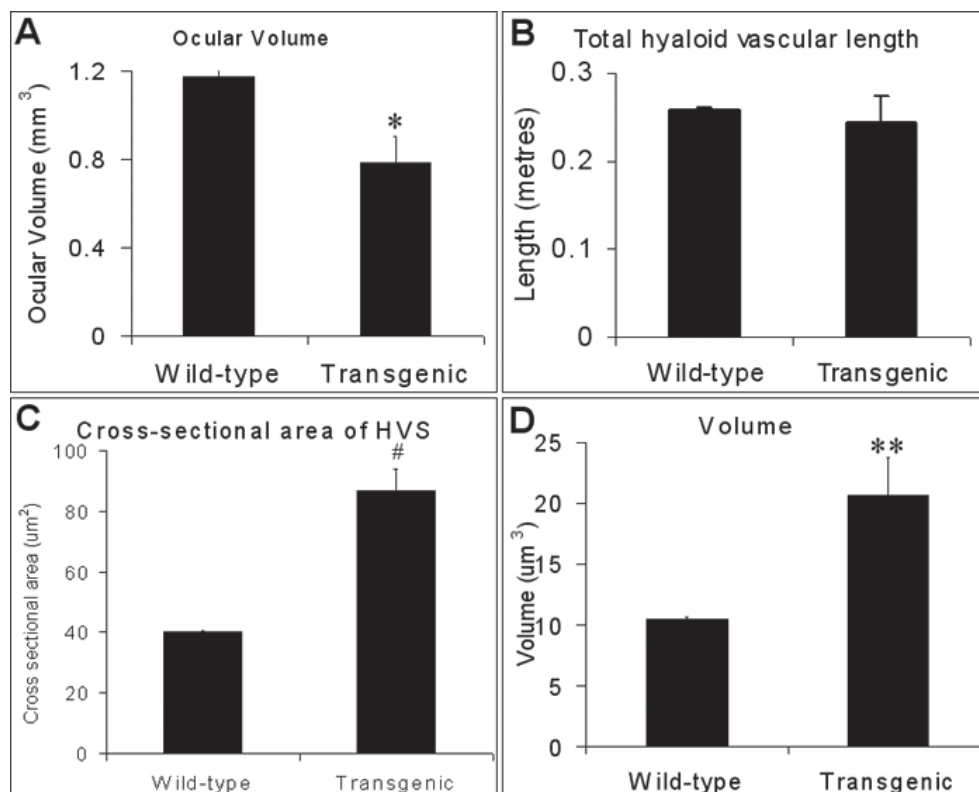

Figure 2. Ocular and hyaloid vascular dimensions in wild-type and VEGF-A_{188} transgenic mice. Total ocular volume (**A**), hyaloid blood vessel length (**B**), cross-sectional area (**C**), and total blood vessel volume (**D**; blood vessel volume=length times cross-sectional area) in E18.5 fetuses from wild-type (n=6) and transgenic (n=5) littermates. Systematic random sampling and stereological methods were used to determine the dimensions of each parameter (see Methods). Statistical analysis was performed using one-way ANOVA with post-hoc testing (SPSS v11.0). The asterisk indicates a p<0.008, the double asterisk indicates a p<0.002, and the sharp (hash mark) indicates a p<0.0001 (wild-type compared to transgenic mice at E18.5). The error bars represent the mean±SEM.

retina, lens capsule, and surrounding the aberrant hyaloid vasculature of E15.5, P1 and adult VEGF-A$_{188}$ transgenic eyes (Figure 3C,E,G, respectively).

HSPG imunohistochemistry: Immunohistochemical staining for HSPG revealed antibody-specific staining in the lens capsules from the eyes of E15.5 wild-type (Figure 3H,I) and VEGF-A$_{188}$ (Figure 3J) transgenic mice. Lens capsules from E15.5 and adult wild-type mice (Figure 3I,K) were considerably thicker and showed a laminar pattern of HSPG immunostaining in comparison to VEGF-A$_{188}$ mice (Figure 3J,L), where lens capsules were attenuated and intensely HSPG immunoreactive. Staining was also conspicuous around the hyaloid vasculature of transgenic mice (Figure 3J,L).

α-smooth muscle actin immunohistochemistry: Specific staining for α-smooth muscle actin (α-SMA) was observed in periendothelial cells located on the ablumenal vascular surfaces of capillaries from both wild-type (Figure 3M,N) and transgenic (Figure 3O) mice. In addition, the numbers of pericytes per vessel, as identified by ultrastructural features, was greater in transgenic than littermate controls (Figure 4).

F4/80 immunohistochemistry: Cells immunostained with the F4/80 antibody, which detects cells from the monocyte/macrophage lineage [23], were observed adhering to the hyaloid vasculatures in both wild-type and VEGF-A$_{188}$ transgenic mice (Figure 3P,Q, respectively).

Cell types comprising the hyaloid vasculature: The hyaloid vasculature is comprised of three primary cell types: endothelium, specialized macrophages (hyalocytes), and pericytes [24]. Ultrastructural features were used to identify these cell types in representative median sagittal sections from both wild-type and VEGF-A$_{188}$ transgenic eyes. There is an increase in the number of endothelial cells and pericytes in transgenic mice compared with littermate controls at E13.5, E15.5, and E17.5 (P<0.0001, Figure 4). Although there is a 2/3 fold increase in both ECs and pericytes, the ratios of these cell types remained relatively constant throughout fetal development. At E13.5 the ratio of EC:pericytes was 3.88:1 (wild-type) and 4.02:1 (transgenic), compared to E15.5 at 5.08:1 (wild-type) and 3.33:1 (transgenic) and E17.5, where the ratio was 3.89:1 (wild-type) and 3.19:1 (transgenic). Although the trend was toward greater numbers of F4/80 positive cells in transgenic mice, we observed no statistical difference compared to littermate controls (p=0.051).

DISCUSSION

Microphthalmia in humans is associated with a range of inherited genetic abnormalities, including microphthalmia with linear skin defects (MLS) syndrome [25], Lenz microphthalmia [26,27], and Norrie's disease [28]. Microphthalmia is frequently observed in infants affected with PHPV [29] and this disorder is also commonly associated with premature birth. In the present study, the characteristic ocular phenotype of VEGF-A$_{188}$ transgenic mice is microphthalmia, cataracts, persistent hyperplastic hyaloid vasculature, lens defects, and retinal hyperplasia. The microphthalmia and cataract formation is also a characteristic specifically observed in VEGF-A$_{188}$ mice. This phenotype was not previously reported in mice overexpressing the more labile VEGF-A$_{165}$ isoform when it was overexpressed from the αA-crystalline promoter [1]. In addition, the HV and lens abnormalities are morphologically distinct when either of these two isoforms (i.e., VEGF-A$_{165}$ [1] or VEGF-A$_{188}$ [this study]) is overexpressed - for example, the reduction in lens size is in contrast to observations made when VEGF-A$_{165}$ was overexpressed from the lens [1], where the lens had expanded

TABLE 1. PROPORTIONS AND TISSUE VOLUMES OF TISSUE TYPES IN WILD-TYPE AND VEGF-A$_{188}$ TRANSGENIC MICE

Tissue		Proportion of tissue (wild-type; n=5)	Proportion of tissue (transgenic; n=6)	Increase/decrease	p value	Volume of tissue (wild-type; n=5)	Volume of tissue (transgenic; n=6)	Increase/decrease	p-value
Retina	A	0.3635±0.0185	0.4903±0.0529	1.35 fold increase	0.03*	0.4386±0.0236	0.3572±0.0203	19% decrease	0.04*
Cornea	B	0.0370±0.0064	0.0454±0.0040	–	0.2	0.0430±0.0064	0.0346±0.0047	–	0.3
Optic Stalk	C	0.0066±0.0010	0.0109±0.0013	1.65 fold increase	0.01*	0.0077±0.0012	0.0080±0.0011	–	0.8
Aqueous	D	0.0026±0.0012	0.0085±0.0044	–	0.1	0.4243±0.0292	0.2215±0.0582	48% decrease	0.01*
Vitreous	E	0.3599±0.0240	0.2611±0.0336	–	0.1	0.0031±0.0013	0.0087±0.0046		0.3
Hyaloid blood vessels (TVL)	F	0.0037±0.0005	0.0148±0.0019	4 fold increase	0.0001*	0.0043±0.0005	0.0110±0.0013	2.56 fold increase	0.001*
Anteria hyaloidea propria (AHP)	G	0.0052±0.0015	0.0115±0.0020	2.2 fold increase	0.003*	0.0061±0.0016	0.0084±0.0013	–	0.3
Iris	H	0.0193±0.0071	0.0336±0.0152	1.7 fold increase	0.02*	0.0229±0.0047	0.0252±0.0031	–	0.6
Lens stroma	I	0.2023±0.0037	0.0779±0.0041	62% decrease	0.004*	0.2387±0.0113	0.0691±0.0212	71% Decrease	0.001*
Lens hemorrhage	J	0±0	0.0460±0.0085	Not observed in wild-type	0.0001*	0±0	0.0406±0.0126	Not observed in wild-type	0.01*
Total Lens	I+J	0.2023±0.0071	0.1239±0.0029	39% decrease	0.01*	0.2387±0.0113	0.1098±0.0337	54% decrease	0.008*
Total Blood Vessels	F+G	0.0089±0.0017	0.0263±0.0027	2.96 fold dncrease	0.0001*	0.0104±0.0019	0.0194±0.0019	1.87 fold increase	0.009*

Proportion of total ocular tissue types in wild-type (n=5) and VEGF-A$_{188}$ transgenic (n=6) mice. Values represent mean±SEM. Statistical comparisons between groups were performed using one-way ANOVA, with significant differences designated by an asterisk. Significance was accepted as p<0.05.

to fill the space within the vitreal and aqueous compartments. Ash and Overbeek [1] suggest that the enlarged lens observed in the VEGF-A$_{165}$ mice may be due to fluid accumulation in the center of the lens. It is possible that reduction in lens size in the VEGF-A$_{188}$ mice resulted from a lack of nutrients and oxygen obtained from the abnormal TVL and that the disrupted lens fiber cell formation also added to the delayed development of the lens.

A significant reduction in lens size, coupled with cataract formation in VEGF-A$_{188}$ transgenic mice, is similar to the phenotype described in rats that are administered with monosodium-L-glutamate on the 9th and 10th day after birth [30].

Small, cataractous lenses are also associated with the "small eyes" (Sey) phenotype, a semidominant, homozygous-lethal mutation in the mouse [31]. The lenticular hemorrhaging observed in the present study parallels that observed in a patient with congenital cataracts. In the aforementioned study, the authors concluded that the cause of the blood clot was a rupture of the anterior end of the hyaloid artery [32] (attached to the posterior lens surface) and that leakage from hyaloid vessels invading the lens nucleus may be responsible for intralenticular bleeding in such eyes [33].

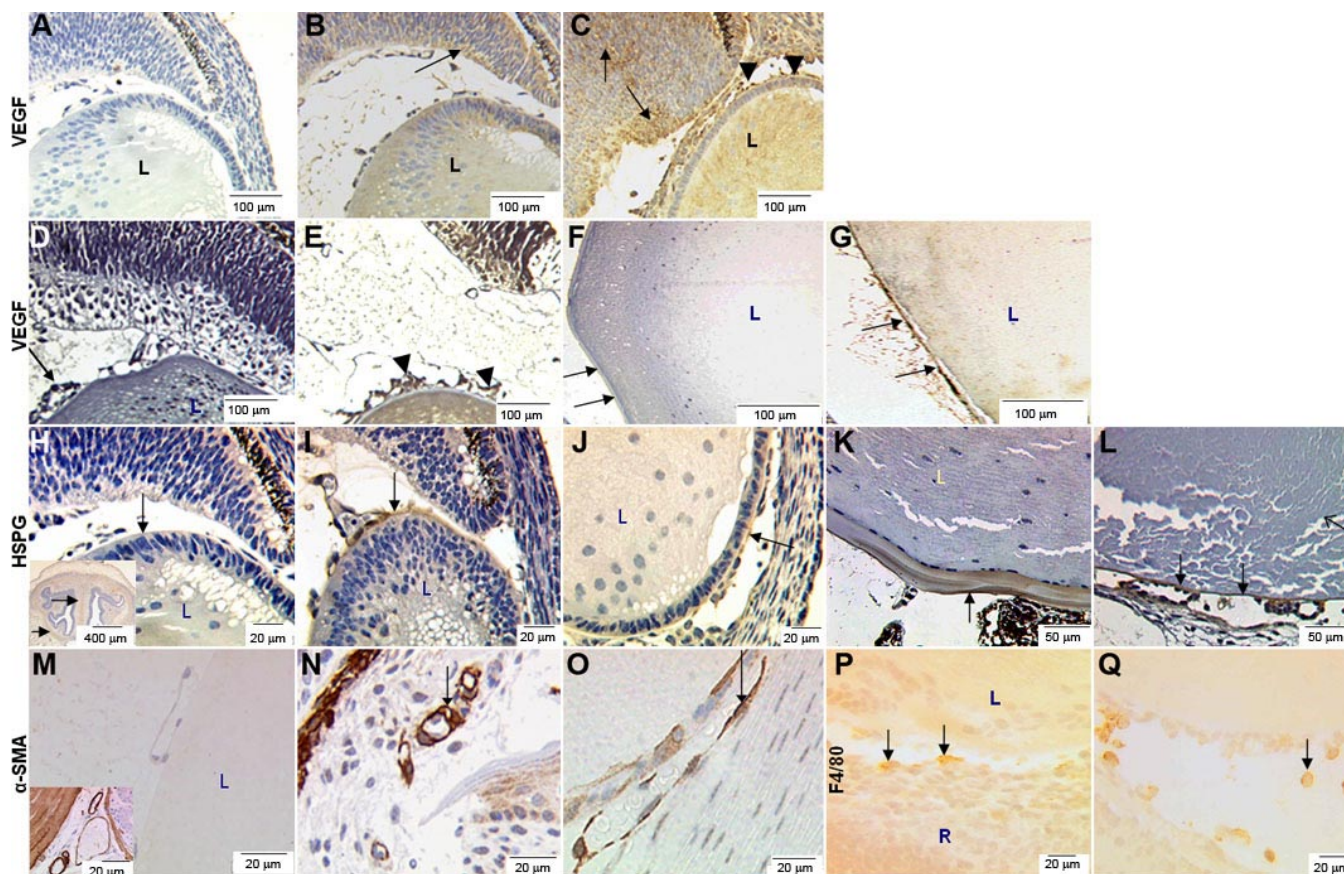It is known that VEGF-A is vital to fetal ocular neovascularization [34], particularly during the formation of

Figure 3. Immunohistochemical detection of VEGF, HSPG, α-SMA, and F4/80 in eyes from wild-type and VEGF-A transgenic mice. Immunohistochemical detection of VEGF-A in wild-type and transgenic mouse eyes at E15.5 (**A-C**), P1 (**D+E**), and adult (**F-G**). **A**; Non-specific IgG serum (control), no discernible background staining is observed. **B**: VEGF-A immunostaining is observed in the wild-type lens (L) and superficial layers of the retina (black arrow) at E15.5. However specific VEGF-A staining was not detected at P1 in the retina, lens, or hyaloid vasculature (**D**). In the adult wild-type eye (**F**), specific staining of the surface of the lens capsule is seen (arrows). Specific staining for VEGF-A is observed in the lens (L), retina (black arrows) and adjacent to the hyaloid vasculature (black arrowheads) at both E15.5 (**C**) and at P1 (**E**) in VEGF-A188 transgenics. In adult VEGF-A188 mice (**G**), prominent staining is observed in the lens capsule (arrows) which appears thinner and (during processing) has separated from the lens structure. Immunohistochemical detection of HSPG (**H-L**), α-SMA (**M-O**), and F4/80 (**P,Q**) in sections from E15.5 (**H-J**, **M-Q**) and adult (**K,L**) mice are shown. **H**: No discernible background staining is observed in control sections (IgG-specific serum). Inset shows an E15.5 mouse brain section, which served as a positive control. **I**: In wild-type mice, specific HSPG staining is observed in the lens capsule and hyaloid vasculature (arrow). **J**: In VEGF-A188 transgenic mice, HSPG staining is observed in the lens capsule (arrow). **K**: HSPG staining is also observed in lens capsule of adult wild-type mice (arrow), with a characteristic laminar pattern. **L**: In adult VEGF-A188 transgenic mice, HSPG staining is seen in the thin lens capsule (arrow) and around persistent hyaloid vasculature (open arrows). Conspicuous staining of peri-vascular smooth muscle cells surrounding blood vessels (arrow) in both E15.5 wild-type (**N**) and transgenic eyes (**O**) was noted. F4/80 immunoreactivity in sections from E15.5 wild- type (**P**) and transgenic mouse eyes (**Q**) revealed cells adjacent to the hyaloid vasculature. In the images, L=lens, R=retina, HV=hyaloid vasculature.

the HV and retinal vasculatures [1,8,35]. VEGF levels are also often elevated in ocular disorders, where increased vascularization is observed [15,17]. In addition, overexpression of human VEGF-A$_{165}$ under the control of the rhodopsin promoter results in a degenerative phenotype characterized by increased retinal vascularization [18]. The doubling of the hyaloid vascular volumes and cross-sectional areas in VEGF-A$_{188}$ mice is consistent with studies in both VEGF-A$_{165}$ overexpressing tumors [36], where vessel fusion resulted in abnormally large lumen formation and also in normally avascular areas in Japanese quail embryos following injection of nanomolar quantities of VEGF-A$_{165}$ at the onset of vasculogenesis [37]. In VEGF-A$_{188}$ transgenic mice (this study), EC number was significantly increased over that in controls from E13.5-E18.5, and these results are consistent with those described for VEGF-A$_{165}$ mice, where proliferation of presumed endothelial precursor cells juxtaposed to the lens was high during the late fetal period and declined thereafter [1]. The concomitant two to three fold increase of both EC and pericyte numbers during late fetal ocular vascularization of VEGF-A$_{188}$ transgenic mice (this study) is consistent with the hypothesis that the proliferation and cell localization of these cell types are intimately linked. VEGF-A is a known mitogen for pericytes [38], and as both ECs and pericytes express VEGF-R2 they are able to respond to this growth factor [39,40]. Previous studies have also shown that VEGF-A promotes maturation of pericytes within the developing retina [41], and that melanoma cells transfected with VEGF-A cDNA promote a strong proliferative response in both pericytes and ECs [42]. Poor blood vessel development has been suggested to be the result of an insufficient population of mesenchymal cells and pericytes to

Figure 4. Numbers of ultrastructurally identified cells within the hyaloid vasculature of wild-type and VEGF-A$_{188}$ transgenic mice. Ultrastructural quantitation of cells in the hyaloid vasculature of VEGF-A$_{188}$ transgenics and control littermates. Quantitation of median coronal sections from E13.5, E15.5, and E17.5 VEGF-A$_{188}$ transgenics and control littermates revealed a consistent 3:1 endothelial cell:pericyte ratio. N=4 per group. WT=wild-type. 188=VEGF-A$_{188}$ transgenic mice.

interact with the overabundance of endothelial cells [1]. This study provides an alternative hypothesis, namely that the pericyte population observed, in both control and VEGF-A$_{188}$ overexpressing mice, increases in tandem with EC number. Hyalocyte (F4/80) positive cells are observed as early as E13.5 in both control and VEGF-A$_{188}$ transgenic mice, in contrast to the low numbers of these cells described in VEGF-A$_{165}$ mice [1]. Hyalocytes are now well known to play a key role in the regression of the hyaloid vasculature, particularly via the expression of Wnt-7b [43]. Our results suggest that the VEGF-A$_{188}$ isoform promotes an increase in hyalocyte numbers, albeit not a statistically significant difference, both within the hyaloid vessel walls and on the ablumenal surface. The role of hyalocytes in the ocular pathology remains to be determined, but the results suggest that as the HV volume increases in VEGF-A$_{188}$ mice, the numbers of hyalocytes do not proportionally increase.

Stereological analysis of VEGF-A$_{188}$ transgenic mice revealed a significantly increased proportion of retina in comparison to wild-type mice, coupled with conspicuous immunolabeling for VEGF in the hypertrophic retina, particularly adjacent to the lens equator. Reduced VEGF-A production in the eye is a cause of retinal thinning [44] and conversely, retinal thickening has been observed in mice with retinal ischemia (associated with increased VEGF-A levels) caused by a surgically increased intraocular pressure [45]. Our data cannot definitively differentiate between retinal hypertrophy resulting from inappropriate neovascularization or as a direct effect of VEGF-A$_{188}$ overexpression on ganglion cell proliferation and differentiation. Overexpression of VEGF-A$_{188}$ from the developing lens also resulted in an increased number of layers in the postnatal cornea of VEGF transgenic mice. One possible explanation for this increased number of EC layers in VEGF-A transgenic corneas is that VEGF-A$_{188}$ transgenic eyes may be subjected to an increased intraocular pressure in relation to the wild-type eye. Several studies have shown that increased intraocular pressure can result in a thickening of the cornea [46-53], however thickening was not observed in our study despite the increase in corneal ECs. Although corneal thickening had not occurred, the properties of the cornea such as protection against noxious agents, biomechanical stability, and structural resiliency as well as the ability to filter out damaging UV light and to aid light refraction may be altered by an increase in density of the cornea. VEGF was originally discovered and termed as vascular permeability factor [54]; therefore, with an increased number of hyaloid blood vessels which are more permeable (as evidenced from the histological and ultrastructural examinations of VEGF-A$_{188}$ transgenic eyes), leakage of serum proteins is highly likely contribute to the ocular pathology we describe.

Previous studies in humans [55] and in mice [1] have demonstrated that VEGF-A is expressed within the lens and supports early fetal lens growth by stimulating the proliferation and migration of angioblasts. In addition to the developmental significance of VEGF-A, a range of ocular pathologies are characterized by inappropriate neovascularization and are coincident with increased levels of VEGF-A. These include pro-
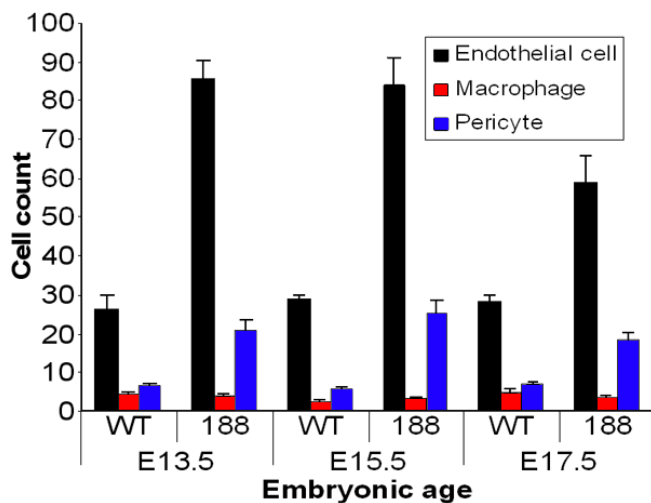
liferative diabetic retinopathy [15,17], age-related macular degeneration [56], retinal neovascularization [18], and retinopathy of prematurity [16]. The immunohistochemical data from this study confirm that VEGF-A is overexpressed within the lens of the transgenic mice and deposited within the lens capsule, where HSPG co-localizes. VEGF-A$_{188}$ has a strong affinity for heparin [12] and the specific lens capsule accumulation of this protein along with HSPG, is consistent with a role for VEGF-A$_{188}$ (and other VEGF-A heparin binding isoforms) in response to wounding. In adult mice and humans, the lens capsule is normally avascular [57], however, following injury such as lens replacement, intense neovascularization surrounding the lens capsule is a common indication for further surgical intervention [58-60]. The presence of HSPG-bound high molecular weight VEGF-A isoforms in the lens may thus prove to be amenable to therapeutic intervention, reducing the incidence of pathological neovascularization.

During normal development of the human eye, the hyaloid vasculature nurtures the developing lens during intrauterine life; in PHPV however, the hyaloid tissue fails to regress and forms a fibrovascular mass behind the lens, resulting in cataracts [29] and bleeding into the vitreous - phenotypes characteristic of the VEGF-A$_{188}$ model. PHPV is a common congenital developmental anomaly of the eye [61], affecting around one in 15,000 live births [62]. Various mammalian species show morphologic features of PHPV, as the disorder has also been reported in cats [63], dogs (where the condition is commonly bilateral [64]), llamas (also bilateral [65]), and in laboratory rats [63], however the etiology of the disorder has not been established. In addition to revealing a role for VEGF-A$_{188}$ in large vessel formation, microphthalmia, lens anomalies and retinal hypertrophy, the VEGF-A$_{188}$ mice described in this study are phenotypically similar to PHPV and should serve as a useful model for preclinical testing of potential therapeutic treatments of this condition.

ACKNOWLEDGEMENTS

REFERENCES

1. Ash JD, Overbeek PA. Lens-specific VEGF-A expression induces angioblast migration and proliferation and stimulates angiogenic remodeling. Dev Biol 2000; 223:383-98.
2. Reneker LW, Overbeek PA. Lens-specific expression of PDGF-A alters lens growth and development. Dev Biol 1996; 180:554-65.
3. Tanaka T, Saika S, Ohnishi Y, Ooshima A, McAvoy JW, Liu CY, Azhar M, Doetschman T, Kao WW. Fibroblast growth factor 2: roles of regulation of lens cell proliferation and epithelial-mesenchymal transition in response to injury. Mol Vis 2004; 10:462-7.
4. Miquerol L, Langille BL, Nagy A. Embryonic development is disrupted by modest increases in vascular endothelial growth factor gene expression. Development 2000; 127:3941-6.
5. Ferrara N, Carver-Moore K, Chen H, Dowd M, Lu L, O'Shea KS, Powell-Braxton L, Hillan KJ, Moore MW. Heterozygous embryonic lethality induced by targeted inactivation of the VEGF gene. Nature 1996; 380:439-42.
6. Carmeliet P, Ferreira V, Breier G, Pollefeyt S, Kieckens L, Gertsenstein M, Fahrig M, Vandenhoeck A, Harpal K, Eberhardt C, Declercq C, Pawling J, Moons L, Collen D, Risau W, Nagy A. Abnormal blood vessel development and lethality in embryos lacking a single VEGF allele. Nature 1996; 380:435-9.
7. Gerber HP, Hillan KJ, Ryan AM, Kowalski J, Keller GA, Rangell L, Wright BD, Radtke F, Aguet M, Ferrara N. VEGF is required for growth and survival in neonatal mice. Development 1999; 126:1149-59.
8. Mitchell CA, Risau W, Drexler HC. Regression of vessels in the tunica vasculosa lentis is initiated by coordinated endothelial apoptosis: a role for vascular endothelial growth factor as a survival factor for endothelium. Dev Dyn 1998; 213:322-33.
9. Ferrara N, Houck K, Jakeman L, Leung DW. Molecular and biological properties of the vascular endothelial growth factor family of proteins. Endocr Rev 1992; 13:18-32.
10. Shima DT, Kuroki M, Deutsch U, Ng YS, Adamis AP, D'Amore PA. The mouse gene for vascular endothelial growth factor. Genomic structure, definition of the transcriptional unit, and characterization of transcriptional and post-transcriptional regulatory sequences. J Biol Chem 1996; 271:3877-83.
11. Leung DW, Cachianes G, Kuang WJ, Goeddel DV, Ferrara N. Vascular endothelial growth factor is a secreted angiogenic mitogen. Science 1989; 246:1306-9.
12. Park JE, Keller GA, Ferrara N. The vascular endothelial growth factor (VEGF) isoforms: differential deposition into the subepithelial extracellular matrix and bioactivity of extracellular matrix-bound VEGF. Mol Biol Cell 1993; 4:1317-26.
13. Ng YS, Rohan R, Sunday ME, Demello DE, D'Amore PA. Differential expression of VEGF isoforms in mouse during development and in the adult. Dev Dyn 2001; 220:112-21.
14. Davies MJ, Mitchell CA, Maley MA, Grounds MD, Harvey AR, Plant GW, Wood DJ, Hong Y, Chirila TV. In vitro assessment of the biological activity of basic fibroblast growth factor released from various polymers and biomatrices. J Biomater Appl 1997; 12:31-56.
15. Sone H, Kawakami Y, Segawa T, Okuda Y, Sekine Y, Honmura S, Segawa T, Suzuki H, Yamashita K, Yamada N. Effects of intraocular or systemic administration of neutralizing antibody against vascular endothelial growth factor on the murine experimental model of retinopathy. Life Sci 1999; 65:2573-80.
16. Zhang W, Ito Y, Berlin E, Roberts R, Luan H, Berkowitz BA. Specificity of subnormal deltaPO2 for retinal neovascularization in experimental retinopathy of prematurity. Invest Ophthalmol Vis Sci 2003; 44:3551-5.
17. Ahmed A, Dunk C, Ahmad S, Khaliq A. Regulation of placental vascular endothelial growth factor (VEGF) and placenta growth factor (PIGF) and soluble Flt-1 by oxygen—a review. Placenta 2000; 21 Suppl A:S16-24.
18. Okamoto N, Tobe T, Hackett SF, Ozaki H, Vinores MA, LaRochelle W, Zack DJ, Campochiaro PA. Transgenic mice with increased expression of vascular endothelial growth factor in the retina: a new model of intraretinal and subretinal neovascularization. Am J Pathol 1997; 151:281-91.
19. Mitchell CA, Rutland CS, Walker M, Nasir M, Foss AJ, Stewart C, Gerhardt H, Konerding MA, Risau W, Drexler HC. Unique

vascular phenotypes following over-expression of individual VEGFA isoforms from the developing lens. Angiogenesis 2006; 9:209-24.

20. Gundersen HJ, Jensen EB. The efficiency of systematic sampling in stereology and its prediction. J Microsc 1987; 147:229-63.

21. Mayhew TM, Burton GJ. Methodological problems in placental morphometry: apologia for the use of stereology based on sound sampling practice. Placenta 1988; 9:565-81.

22. Saint-Geniez M, D'Amore PA. Development and pathology of the hyaloid, choroidal and retinal vasculature. Int J Dev Biol 2004; 48:1045-58.

23. Leenen PJ, de Bruijn MF, Voerman JS, Campbell PA, van Ewijk W. Markers of mouse macrophage development detected by monoclonal antibodies. J Immunol Methods 1994; 174:5-19.

24. Zhu M, Provis JM, Penfold PL. The human hyaloid system: cellular phenotypes and inter-relationships. Exp Eye Res 1999; 68:553-63.

25. Morleo M, Pramparo T, Perone L, Gregato G, Le Caignec C, Mueller RF, Ogata T, Raas-Rothschild A, de Blois MC, Wilson LC, Zaidman G, Zuffardi O, Ballabio A, Franco B. Microphthalmia with linear skin defects (MLS) syndrome: clinical, cytogenetic, and molecular characterization of 11 cases. Am J Med Genet A 2005; 137:190-8.

26. Ng D, Hadley DW, Tifft CJ, Biesecker LG. Genetic heterogeneity of syndromic X-linked recessive microphthalmia-anophthalmia: is Lenz microphthalmia a single disorder? Am J Med Genet 2002; 110:308-14.

27. Ng D, Thakker N, Corcoran CM, Donnai D, Perveen R, Schneider A, Hadley DW, Tifft C, Zhang L, Wilkie AO, van der Smagt JJ, Gorlin RJ, Burgess SM, Bardwell VJ, Black GC, Biesecker LG. Oculofaciocardiodental and Lenz microphthalmia syndromes result from distinct classes of mutations in BCOR. Nat Genet 2004; 36:411-6.

28. Berger W. Molecular dissection of Norrie disease. Acta Anat (Basel) 1998; 162:95-100.

29. Khaliq S, Hameed A, Ismail M, Anwar K, Leroy B, Payne AM, Bhattacharya SS, Mehdi SQ. Locus for autosomal recessive nonsyndromic persistent hyperplastic primary vitreous. Invest Ophthalmol Vis Sci 2001; 42:2225-8.

30. Kawamura M, Azuma N. Morphological studies on cataract and small lens formation in neonatal rats treated with monosodium-L-glutamate. Ophthalmic Res 1992; 24:289-97.

31. Roberts SR. Color dilution and hereditary defects in collie dogs. Am J Ophthalmol 1967; 63:1762-75.

32. Unoki K, Nakao K, Ohba N. Haemorrhage in the lens: spontaneous occurrence in congenital cataract. Br J Ophthalmol 1986; 70:593-5.

33. Federman JL, Shields JA, Altman B, Koller H. The surgical and nonsurgical management of persistent hyperplastic primary vitreous. Ophthalmology 1982; 89:20-4.

34. Neely KA, Gardner TW. Ocular neovascularization: clarifying complex interactions. Am J Pathol 1998; 153:665-70.

35. Gerhardt H, Golding M, Fruttiger M, Ruhrberg C, Lundkvist A, Abramsson A, Jeltsch M, Mitchell C, Alitalo K, Shima D, Betsholtz C. VEGF guides angiogenic sprouting utilizing endothelial tip cell filopodia. J Cell Biol 2003; 161:1163-77.

36. Benjamin LE, Keshet E. Conditional switching of vascular endothelial growth factor (VEGF) expression in tumors: induction of endothelial cell shedding and regression of hemangioblastoma-like vessels by VEGF withdrawal. Proc Natl Acad Sci U S A 1997; 94:8761-6.

37. Drake CJ, Little CD. Exogenous vascular endothelial growth factor induces malformed and hyperfused vessels during embryonic neovascularization. Proc Natl Acad Sci U S A 1995; 92:7657-61.

38. Hagedorn M, Balke M, Schmidt A, Bloch W, Kurz H, Javerzat S, Rousseau B, Wilting J, Bikfalvi A. VEGF coordinates interaction of pericytes and endothelial cells during vasculogenesis and experimental angiogenesis. Dev Dyn 2004; 230:23-33.

39. Giavazzi R, Sennino B, Coltrini D, Garofalo A, Dossi R, Ronca R, Tosatti MP, Presta M. Distinct role of fibroblast growth factor-2 and vascular endothelial growth factor on tumor growth and angiogenesis. Am J Pathol 2003; 162:1913-26.

40. Witmer AN, van Blijswijk BC, van Noorden CJ, Vrensen GF, Schlingemann RO. In vivo angiogenic phenotype of endothelial cells and pericytes induced by vascular endothelial growth factor-A. J Histochem Cytochem 2004; 52:39-52.

41. Fruttiger M. Development of the mouse retinal vasculature: angiogenesis versus vasculogenesis. Invest Ophthalmol Vis Sci 2002; 43:522-7.

42. Kusters B, Leenders WP, Wesseling P, Smits D, Verrijp K, Ruiter DJ, Peters JP, van Der Kogel AJ, de Waal RM. Vascular endothelial growth factor-A(165) induces progression of melanoma brain metastases without induction of sprouting angiogenesis. Cancer Res 2002; 62:341-5.

43. Lobov IB, Rao S, Carroll TJ, Vallance JE, Ito M, Ondr JK, Kurup S, Glass DA, Patel MS, Shu W, Morrisey EE, McMahon AP, Karsenty G, Lang RA. WNT7b mediates macrophage-induced programmed cell death in patterning of the vasculature. Nature 2005; 437:417-21.

44. Haigh JJ, Morelli PI, Gerhardt H, Haigh K, Tsien J, Damert A, Miquerol L, Muhlner U, Klein R, Ferrara N, Wagner EF, Betsholtz C, Nagy A. Cortical and retinal defects caused by dosage-dependent reductions in VEGF-A paracrine signaling. Dev Biol 2003; 262:225-41.

45. Chen YG, Zhang C, Chiang SK, Wu T, Tso MO. Increased nuclear factor-kappa B p65 immunoreactivity following retinal ischemia and reperfusion injury in mice. J Neurosci Res 2003; 72:125-31.

46. Pico JF, Stamper RL, McMenemy M. Intraocular pressure and corneal curvature changes on application of limbal-scleral suction fixation ring in rabbits. Cornea 1993; 12:25-8.

47. Setala K, Vannas A. Corneal endothelial cells in essential iris atrophy. A specular microscipic study. Acta Ophthalmol (Copenh) 1979; 57:1020-9.

48. Herndon LW, Choudhri SA, Cox T, Damji KF, Shields MB, Allingham RR. Central corneal thickness in normal, glaucomatous, and ocular hypertensive eyes. Arch Ophthalmol 1997; 115:1137-41.

49. Copt RP, Thomas R, Mermoud A. Corneal thickness in ocular hypertension, primary open-angle glaucoma, and normal tension glaucoma. Arch Ophthalmol 1999; 117:14-6.

50. Brusini P, Miani F, Tosoni C. Corneal thickness in glaucoma: an important parameter? Acta Ophthalmol Scand Suppl 2000; 78:41-2.

51. Brandt JD, Beiser JA, Kass MA, Gordon MO. Central corneal thickness in the Ocular Hypertension Treatment Study (OHTS). Ophthalmology 2001; 108:1779-88.

52. Herman DC, Hodge DO, Bourne WM. Increased corneal thickness in patients with ocular hypertension. Arch Ophthalmol 2001; 119:334-6.

53. Singh RP, Goldberg I, Graham SL, Sharma A, Mohsin M. Central corneal thickness, tonometry, and ocular dimensions in glau-

coma and ocular hypertension. J Glaucoma 2001; 10:206-10.

54. Senger DR, Galli SJ, Dvorak AM, Perruzzi CA, Harvey VS, Dvorak HF. Tumor cells secrete a vascular permeability factor that promotes accumulation of ascites fluid. Science 1983; 219:983-5.

55. Gogat K, Le Gat L, Van Den Berghe L, Marchant D, Kobetz A, Gadin S, Gasser B, Quere I, Abitbol M, Menasche M. VEGF and KDR gene expression during human embryonic and fetal eye development. Invest Ophthalmol Vis Sci 2004; 45:7-14.

56. Lip PL, Blann AD, Hope-Ross M, Gibson JM, Lip GY. Age-related macular degeneration is associated with increased vascular endothelial growth factor, hemorheology and endothelial dysfunction. Ophthalmology 2001; 108:705-10.

57. Tripathi RC, Tripathi BJ. Lens morphology, aging, and cataract. J Gerontol 1983; 38:258-70.

58. Pangtey MS, Khokhar S, Sony P, Panda A, Sethi HS, Chandra P. Posttraumatic neovascularization in a cataractous crystalline lens. J Cataract Refract Surg 2003; 29:859-60; author reply 860-1.

59. Hwang YS, Lai CC, Lee JS, Yang KJ, Chen TL. Posttraumatic neovascularization in a cataractous crystalline lens. J Cataract Refract Surg 2002; 28:715-6.

60. Bene C, Hutchins R, Kranias G. Cataract wound neovascularization. An often overlooked cause of vitreous hemorrhage. Ophthalmology 1989; 96:50-3.

61. Silbert M, Gurwood AS. Persistent hyperplastic primary vitreous. Clin. Eye Vis. Care 2000; 12:131-137.

62. Reichel MB, Ali RR, D'Esposito F, Clarke AR, Luthert PJ, Bhattacharya SS, Hunt DM. High frequency of persistent hyperplastic primary vitreous and cataracts in p53-deficient mice. Cell Death Differ 1998; 5:156-62.

63. Allgoewer I, Pfefferkorn B. Persistent hyperplastic tunica vasculosa lentis and persistent hyperplastic primary vitreous (PHTVL/PHPV) in two cats. Vet Ophthalmol 2001; 4:161-4.

64. Bayon A, Tovar MC, Fernandez del Palacio MJ, Agut A. Ocular complications of persistent hyperplastic primary vitreous in three dogs. Vet Ophthalmol 2001; 4:35-40.

65. Gionfriddo JR, Blair M. Congenital cataracts and persistent hyaloid vasculature in a llama (Lama glama). Vet Ophthalmol 2002; 5:65-70.